Narrow-Band and Low-Loss Bandpass Filter for Quasi Millimeter-wave 5G Application

Yusuke Uemichi,[1] Shinnosuke Tsuchiya,[1] Toru Yamaguchi,[1]
Xu Han,[1] Osamu Nukaga,[1] Shuhei Amakawa,[2] and Ning Guan [1]

A 28-GHz bandpass filter (BPF) with a 2-GHz bandwidth (7% fractional bandwidth) built of silica-based post-wall waveguide (PWW) is presented for 5G-applications. The filter is composed of 5 cylindrical resonators. The dielectric loss-tangent of the substrate is as low as 0.00036 at 44 GHz. The dimensions of the BPF is 11×10 mm². The insertion loss of the BPF, not including I/O interfaces for probing measurement, is less than 0.8 dB. Design of I/O interfaces for the BPF is also presented.

1. Introduction

In recent years, 5G wireless systems are being realized at frequencies below 6 GHz and technologies applying millimeter-wave (mmWave) frequencies such as 28 GHz- and 39 GHz- bands will play indispensable role in the near future. Among the key components for 5G applications, bandpass filters (BPFs) are very important and definitely necessary. They cannot be designed based on traditional technologies such as SAW or BAW devices and should be designed based on distributed-element circuit directly in the mmWave frequencies. But there are very few reports about BPFs targeting these frequency bands. [1)2)] Especially, no 28-GHz BPF with a bandwidth narrower than 2 GHz seems to have been reported as yet. In order to realize low-loss filter with sharp out-of-band rejection, choice of material is very important because High-Q resonator is essential for the filter. Moreover, very high processing accuracy is also essential for realization of narrow-band filter. We believe silica-based post-wall waveguide (PWW) technology is the most promising technology as the solution. We reported potential of millimeter-wave devices built of very low-loss silica-based post-wall waveguide (PWW) for 60-GHz band and E-band . [3) 4) 5) 6) 7) 8)] In this paper, we present the feasibility of a narrow band five-stage Chebyshev BPF built of silica-based PWW for 28 GHz applications.

2. Waveguide and I/O interfaces

To evaluate PWWs and BPFs built thereof, we need to realize I/O interfaces. We chose synthetic fused silica as the material of the substrate. The measured relative dielectric constant ε_r and dielectric loss tangent tanδ were 3.82 and 0.00036, respectively, at 44 GHz. The width of the waveguide was determined to be 4.0 mm so that 29.5 GHz becomes 1.5 times the cut-off frequency of the TE_{10} mode. The diameter of the posts and the spacing between them are 100 μm and 200 μm, respectively. Substrate thickness was chosen as 860 μm. Figure 1 shows the concept of I/O interface. A blind-via is applied to excite dominant TE_{10} mode into the PWW. [9) 10) 11)] In principle, wideband operation is achievable by using a single blind-via. But the required depth of between 600 μm and 700 μm makes its aspect ratio too high, giving rise to poor manufacturing yield. So we, instead, used a bundle of 5 blind-vias. Figure 2 shows the bundle. As shown in Fig. 3, 5 blind-vias are arranged to have four-fold symmetry. The depth of the center blind-via is 775 μm and that of the others are 725 μm. The proposed I/O interfaces enable us to connect planar circuits such as ICs and bulky PWWs.

3. Fabrication and evaluation

Figure 4 shows bird's eye view of the fabricated bundle of blind-vias. A copper strip is connected to the bundle and most part of it runs over the cutout, leading to a pad for probing.

Figure 5 shows cross-sectional side views of the fabricated bundle of blind-vias. Figure 6 shows the concept of test structure of PWW. The test structure has two blind-vias with pads for the input and output terminal for 2-port probing measurement. Figure 7 shows the top view of fabricated test structures. We prepared PWWs having 3 different lengths (6 mm, 12 mm and 18 mm). Figure 8 shows the measured |S11| for the 20 6-mm-long samples. It shows good performance at the frequencies between 22 GHz and 32 GHz. The waveguide with I/O interfaces sufficiently cover the frequencies between 24 GHz and 30 GHz required for 5G communication. We found that the tip of the bundle was split into 5, which was different from the intended design, and that the substrate thickness was 19 μm thinner than the designed value as shown in Fig.5. Nevertheless, we confirmed high yield and good electrical characteristics by measurements. Figure 9

1 : Electronic Technologies R&D Center, Fujikura Ltd, Japan
2 : Graduate School of Advanced Sciences of Matter, Hiroshima University, Japan

Panel 1. Abbreviations, Acronyms, and Terms.

PWW—Post-Wall Waveguide
SAW—Surface Acoustic Wave filter
BAW—Bulk Acoustic Wave filter

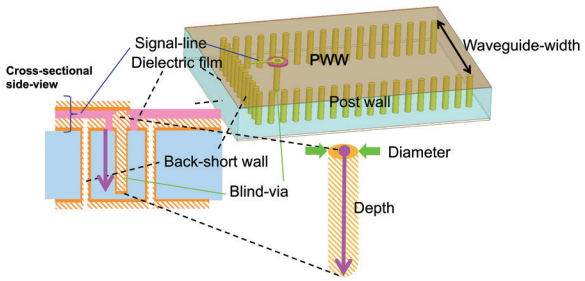

Fig.1. I/O interface for PWW.

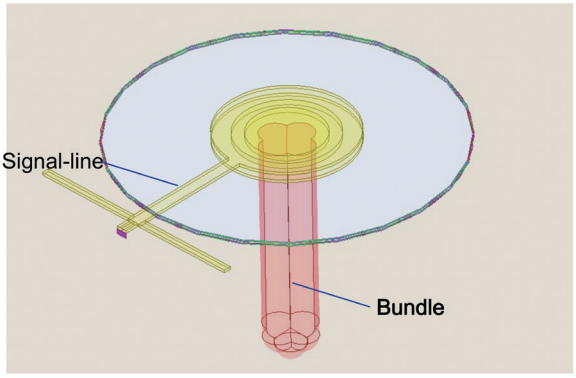

Fig.2. Proposed I/O interface by a bundle of 5 blind-vias.

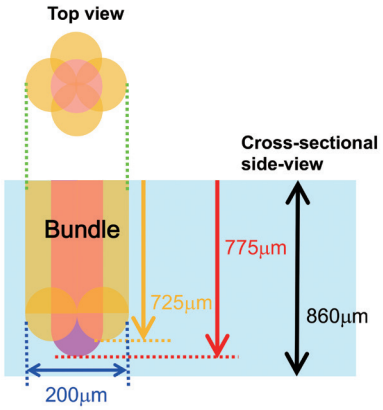

Fig.3. A designed bundle of 5 blind-vias for TE_{10} excitation.

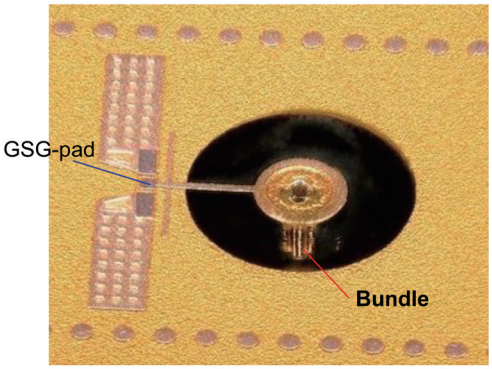

Fig.4. Fabricated blind-vias based I/O interfaces.

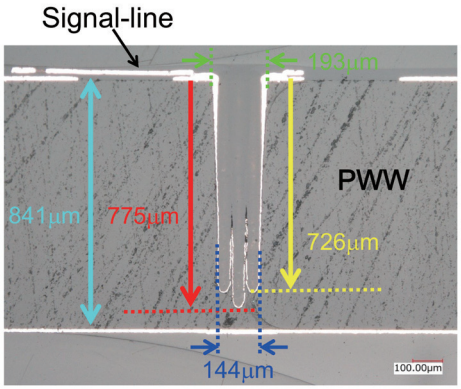

Fig.5. Cross-sectional side view of the fabricated blind-vias based I/O interfaces.

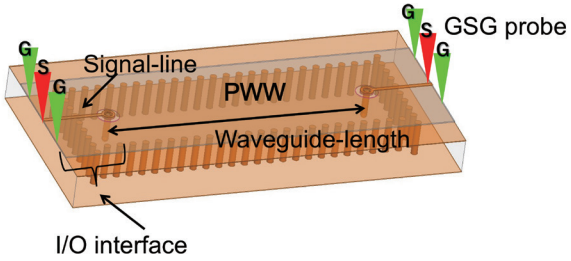

Fig.6. Test structure of PWW.

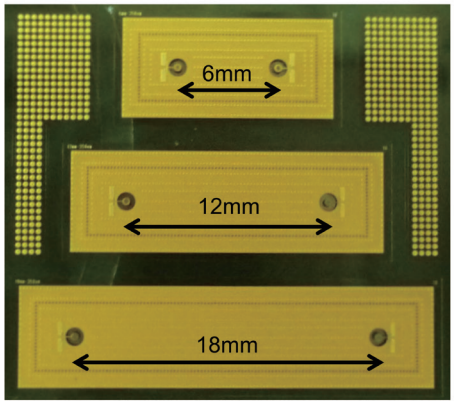

Fig.7. Fabricated test structures of PWW.

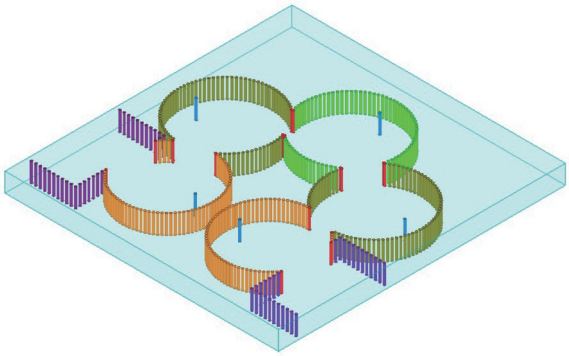

Fig.10. Proposed geometry of bandpass filter.

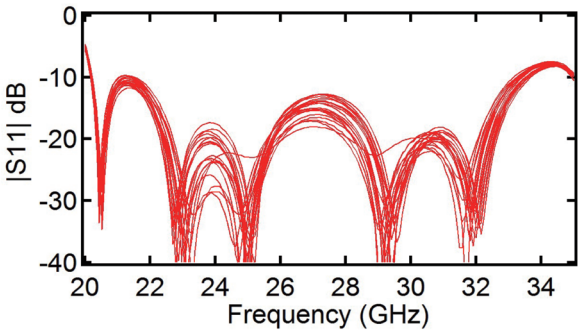

Fig.8. Measured |S11| of 6 mm- PWW with blind-vias based I/O interfaces.

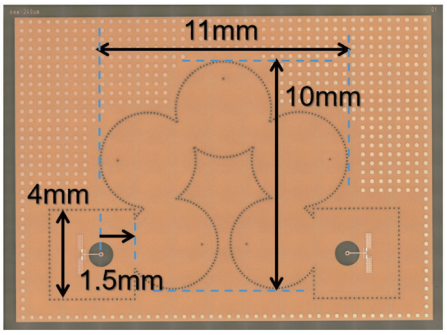

Fig.11. Fabricated bandpass filter.

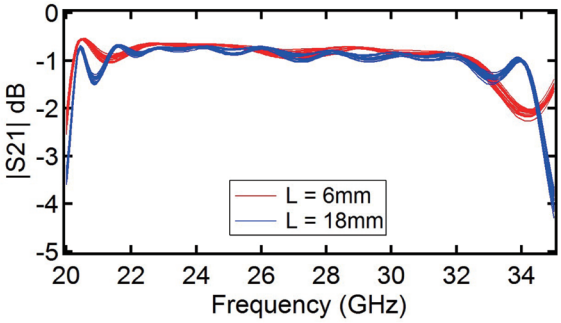

Fig.9. Measured |S21| of 6 mm- and 18 mm- PWW with blind-vias based I/O interfaces.

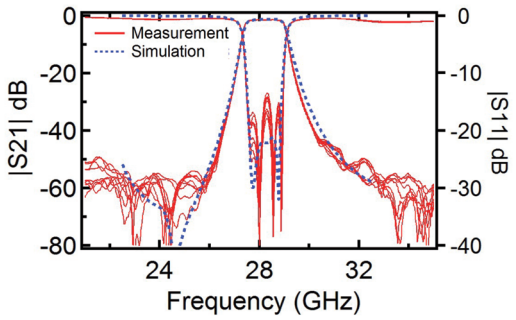

Fig.12. Measured and simulated results of bandpass filter.

shows the measured |S21| for the 6-mm-long and 18-mm-long samples. We intended to estimate the loss of PWW and I/O interface by the relationship between waveguide-length and measured |S21|. [9) 10)] The PWW is so low-loss that it was difficult to distinguish the loss magnitudes between the 6-mm-long and 18-mm-long PWWs. Neglecting the loss of PWW, the loss of a pair of I/O interfaces can be estimated to be about 0.8 dB.

4. Bandpass filter

We tried to design 28-GHz BPF with 2-GHz bandwidth which seems not to have been reported as yet. According to 12), it is known that insertion-loss of BPF is in inverse proportion to the fractional bandwidth (FBW). Therefore, it is difficult to realize low-loss and narrow-band BPF because the narrower the FBW, the higher insertion loss becomes. The choice of low-loss material is very important because high-Q resonators are essential for

realization of low-loss and narrow-band BPF. We designed a five-stage Chebyshev-type BPF based on n = 5 and 0.5 dB ripples. The pass-band is from 27.5 GHz to 29.5 GHz, with the fractional bandwidth (FBW) being 7%. The element values of the prototype low-pass filter gi, are $g1$ = $g5$ = 1.7058, $g2$ = $g4$ = 1.2296 and $g5$ = 2.5408. The values of the coupling coefficients $m$ij between the ith and jth resonant cavities are $m12$ = $m45$ = 0.0485, $m23$ = $m34$ = 0.0397. The external quality factors are Q_{es} = Q_{eL} = 24.3. Figure 10 shows the geometry of the proposed BPF. The filter is realized as direct coupled resonator filter and is composed of 5 cylindrical resonators arranged symmetrically. We controlled the distance between 2 cylindrical resonators to obtain intended coupling "$m$ij". The control of coupling between resonators affects resonant frequency of each resonator at the same time. But the resonant frequency of each resonator should be identical and it makes filter design difficult. To relieve the difficulty, each of the cylindrical resonators in the proposed BPF has a metalized through hole, the position of which allows the resonant frequency to be tuned. [13] As a result, the radii of the resonators are nearly equal to 2 mm.

Figure 11 shows the fabricated BPF. The intrinsic dimensions of the BPF are 11 mm by 10 mm.

The bundle for TE_{10} excitation was placed very close to the coupling windows of the first and fifth resonators. Figure 12 shows the measured and simulated S-parameters for 9 samples. The red solid lines indicate measured results and the blue dotted lines are the simulation results.

The simulation model is shown in Fig.10 and it does not include I/O interfaces. In contrast, the measured BPF includes I/O interfaces which are placed very close to the coupling windows of the first and fifth resonators. Despite these facts, the measured BPF performance was nearly perfectly as designed, which shows high-accuracy of design and effectiveness of the proposed I/O interfaces. The pass-band insertion loss ranges from 1.3 dB to 1.6 dB. If the loss due to I/O interfaces is 0.8 dB as described in the previous section, the intrinsic insertion loss of the BPF can be estimated to range from 0.5 dB to 0.8 dB. From the relationship between the insertion loss of BPF and the resonator quality factor described in 12), the quality factors of cylindrical resonators are estimated to range from 805 to 1290.

5. Conclusion

We realized a narrow-band and low-loss bandpass filter (BPF) for 5G applications. The BPF is based on cylindrical resonators built into a silica-based post-wall waveguide (PWW). We showed that the performance and repeatability are very good and measurement results agree with simulated ones very well. We successfully showed the feasibility of our silica-based PWW technology for quasi-millimeter wave frequencies, which will be used for 5G. This will be the first report on a BPF with a pass-band width of 2 GHz, which is important for 5G. This BPF technology is also applicable to higher frequency bands that are to be used for 5G.

References

1) K. Matsutani, H Kojima, M. Nakahori, K. Kuroda, K. Onaka, M. Koshino, and T. Toi, "Miniaturized quartz waveguide filter using double-folded structure," in IEEE MTT-S Int. Microw. Symp. Dig., pp. 1201–1204. Jun. 2019.
2) M. Ali, F. Liu, A. Watanabe, P. M. Raj, V. Sundaram, M. M. Tentzeris, and R. R. T μmmala, "First demonstration of compact, ultra-thin low-pass and bandpass filters for 5G small-cell applications," IEEE Microw. Wireless Compon. Lett., vol. 28, pp. 1110–1112, Dec. 2018.
3) Y. Uemichi, O. Nukaga, X. Han, R. Hosono, N. Guan and S. Amakawa,"Characterization of 60- GHz silica-based post-wall waveguide and low-loss substrate dielectric," in Proc. Asia-Pacific Microw. Conf., pp. 1–4, Dec 2016.
4) Y. Uemichi, O. Nukaga, K. Nakamura, X. Han, R. Hosono, N. Guan and S. Amakawa, "Compact and low-loss bandpass filter realized in silica-based post-wall waveguide for 60- GHz application," in IEEE MTT-S Int. Microw. Symp. Dig., pp. 1–3. Jun. 2014.
5) Y. Uemichi, O. Nukaga, K. Nakamura, X. Han, R. Hosono, K. Kobayashi and N. Guan, "A 60- GHz six-pole quasi-elliptic bandpass filter with novel feeding mechanisms based on silica-based post-wall waveguide," in IEEE MTT-S Int. Microw. Symp. Dig., pp. 1–3. Jun. 2017.
6) Y. Uemichi, O. Nukaga, K. Nakamura, X. Han, Y. Hasegawa, R. Hosono, K. Kobayashi, N. Guan and S. Amakawa, "An E-band hybridcoupled diplexer built of silica-based post-wall waveguide," in Proc. Eur. Microw. Conf., pp. 819–822, Oct 2017.
7) Y. Uemichi, O. Nukaga, X. Han, K. Kobayashi, S. Amakawa and N. Guan, "Temperature dependence of bandpass filters built of silica-based post-wall waveguide for millimeter-wave applications," in Proc. Eur. Microw. Conf., pp. 703–706, Sept. 2018.
8) Y. Uemichi, O. Nukaga, X. Han, S. Amakawa and N. Guan,, "Highly configurable cylindrical-resonator-based bandpass filter built of silica-based post-wall waveguide and its application to compact E-band hybrid-coupled diplexer," in IEEE MTT-S Int. Microw. Symp. Dig., pp. 726–729. Jun. 2019.
9) Y. Uemichi, O. Nukaga, K. Nakamura, X. Han, R. Hosono and N. Guan,"A ultra low-loss silica-based transformer between microstrip line and post-wall waveguide for millimeter-wave antenna-in-package applications," in IEEE MTT-S Int. Microwave Symp. Dig., pp. 13, Jun. 2014.
10) Y. Uemichi, O. Nukaga, K. Nakamura, X. Han, R. Hosono and N. Guan, "Silica-based post-wall waveguide with high-performance input and output transitions for E-band passive front-end," 2015 Int. Symp. on Antennas and Propagation (ISAP), pp. 1–3, Nov. 2015.
11) Y. Uemichi, O. Nukaga, K. Nakamura, X. Han, R. Hosono and N. Guan, "A study on the broadband transitions between microstrip line and post-wall

waveguide in E-band," in Proc. Eur. Microw. Conf., pp. 13–16, Oct. 2016.
12) J. -S. Hong and M. J. Lancaster, Microstrip Filter for RF/Microwave Applications, Wiely, 2001, ch. 3, sec. 3. 6. 3, p. 73
13) Y. Uemichi, S. Tsuchiya, T. Yamaguchi, X. Han, O. Nukaga, S. Amakawa and N. Guan, "Narrow-band and low-loss bandpass filter for 5G built of Silica-based post-wall waveguide," in Proc. Eur. Microw. Conf., pp. 559–562, Jan. 2021.